Molecular Pharmacology Fast Forward. Published on January 22, 2014 as doi:10.1124/mol.113.091488

Mol Manuscript # 91488

Title: Regulation of GluA1 AMPA receptor function by protein kinase C at Serine-818 and Threonine-840

Authors: Meagan A. Jenkins, Gordon Wells, Julia Bachman, James P. Snyder, Andrew Jenkins, Richard L. Huganir, Robert E. Oswald, Stephen F. Traynelis

Affiliations:
Department of Pharmacology, Emory University, School of Medicine, Atlanta, GA: MAJ, AJ, SFT

Department of Anesthesiology, Emory University, School of Medicine, Atlanta, GA: AJ

Department of Chemistry, Emory University, Atlanta, GA: GW, JPS

Department of Neuroscience and Howard Hughes Medical Institute, Johns Hopkins University School of Medicine, Baltimore, MD: JB, RLH

Department of Molecular Medicine, Cornell University, Ithaca, NY: REO

Molecular Pharmacology Fast Forward. Published on January 22, 2014 as DOI: 10.1124/mol.113.091488
This article has not been copyedited and formatted. The final version may differ from this version.

Running Title: C-terminal regulation of AMPA receptor conductance

Correspondence should be addressed to
Stephen F. Traynelis
1510 Clifton Rd.
Department of Pharmacology, Rollins Research Center
Emory University School of Medicine
Atlanta, GA. 30322
strayne@emory.edu

Number of pages: 44
Numbers of figures: 5
Numbers of tables: 4
Number of words in abstract: 148
Number of words in introduction: 500
Number of words in discussion: 1,076

Abbreviations:

AMPA, α-Amino-3-hydroxy-5-methyl-4-isoxazolepropionic acid; CaMKII, Ca^{2+}-dependent protein kinase II; CMV, cytomegalovirus; COSY, correlation spectroscopy; DL-APV, (*R,S*)-2-amino-5-phosphonovaleric acid; DMEM, Dulbecco's modified Eagle's medium; γ_{MEAN}, weighted mean conductance; GAPDH, glyceraldehydes 3-phosphate dehydrogenase; HEK, human embryonic kidney 293 cells; HSQC, heteronuclear single quantum adherence; LTP, long-term potentiation (LTP); NBQX, 2,3-dihydroxy-6-nitro-7-sulfamoyl-benzo[f]quinoxaline-2,3-dione; NOE, nuclear Overhauser effect; NOESY, nuclear Overhauser effect spectra; PDZ, post synaptic density protein; PMA, phorbol 12-myristate 13-acetate; PSD95, Drosophila disc large tumor suppressor (Dlg1) and zonula occludens-1 protein (zo-1); PKC, Ca^{2+}/phospholipid-dependent protein kinase; (P_O), open probability; ROESY, rotating-frame nuclear Overhauser effect correlation spectra; SS/PK represents the ratio of the steady state (SS) to the peak (PK) current amplitude; TOCSY, total correlated spectra

Molecular Pharmacology Fast Forward. Published on January 22, 2014 as DOI: 10.1124/mol.113.091488
This article has not been copyedited and formatted. The final version may differ from this version.

Abstract

Three residues within the AMPA receptor subunit GluA1 C-terminus (Ser818, Ser831, Thr840) can be phosphorylated by PKC. Here we show that PKC phosphorylation of GluA1 Ser818 or Thr840 enhances the weighted mean channel conductance without altering response time course or agonist potency. These data support the idea that these residues constitute a hyper-regulatory domain for the AMPA receptor. Introduction of phosphomimetic mutations increase conductance only at these three sites within the proximal C-terminus, consistent with a structural model with a flexible linker connecting the distal C-terminal domain to the more proximal domain containing a helix bracketed by Ser831 and Thr840. NMR spectra support this model and raise the possibility that phosphorylation can alter the configuration of this domain. Our findings provide insight into the structure and function of the C-terminal domain of GluA1, which controls AMPA receptor function and trafficking during synaptic plasticity in the central nervous system.

Molecular Pharmacology Fast Forward. Published on January 22, 2014 as DOI: 10.1124/mol.113.091488
This article has not been copyedited and formatted. The final version may differ from this version.

Introduction

Increased intracellular Ca^{2+} following activation of synaptic NMDA receptors activates signaling cascades that induce changes in synaptic strength. One such change, NMDA receptor-dependent long-term potentiation (LTP) of excitatory postsynaptic currents (EPSCs), is hypothesized to be a cellular correlate of memory (Bliss and Collingridge, 1993; Malinow, 1994). A critical target of Ca^{2+}-dependent second messengers active during LTP is the AMPA receptor (Malinow and Malenka, 2002; Song and Huganir, 2002; Kessels and Malinow, 2009). Interactions within the intracellular C-terminal domain regulate AMPA receptor trafficking and gating (Derkach et al., 1999; Banke et al., 2000; Malinow and Malenka, 2002; Poncer et al., 2002; Esteban et al., 2003; Boehm et al., 2006a; Boehm et al., 2006b; Lin and Huganir, 2007; Thomas et al., 2008; Lin et al., 2009; Kristensen et al., 2011). Ca^{2+}-dependent protein kinase II (CaMKII) and Ca^{2+}/phospholipid-dependent protein kinase (PKC) are important during LTP and phosphorylate 3 residues in the GluA1 AMPA receptor C-terminus: GluA1-Ser818, GluA1-Ser831 and GluA1-Thr840 (Hu et al., 1987; Silva et al., 1992; Roche et al., 1996; Barria et al., 1997a; Barria et al., 1997b; Mammen et al., 1997; Ouyang et al., 1999; Ramakers et al., 1999; Poncer et al., 2002; Boehm et al., 2006b; Lee et al., 2007; Lin et al., 2009). Phosphorylation of GluA1-Ser831 is critical for memory retention, expression of LTP and LTD (Lee et al., 2003; Lee et al., 2010; Makino et al., 2011, Lee et al., 2013). Phosphorylation of GluA1-Ser818 by PKC is increased during LTP in hippocampal slices (Boehm et al., 2006b). Phosphorylation of GluA1-Ser818 promotes synaptic incorporation of AMPA receptors, shown using fluorescence microscopy in hippocampal and cortical neurons (Lin et al., 2009). GluA1-Thr840 is phosphorylated by PKC to regulate synaptic plasticity in an age-dependent manner (Lee et al., 2007).

Molecular Pharmacology Fast Forward. Published on January 22, 2014 as DOI: 10.1124/mol.113.091488
This article has not been copyedited and formatted. The final version may differ from this version.

AMPA receptors exhibit subunit-dependent gating in which activation of each agonist-bound subunit incrementally contributes to channel conductance. Higher conductance levels reflect simultaneous gating of multiple subunits, with the highest conductance attained when all four subunits are activated (Rosenmund et al., 1998; Jin et al., 2003; Prieto and Wollmuth, 2010; Poon et al., 2011). Phosphorylation of GluA1-Ser831 enhances AMPA receptor function (Tavalin, 2008) via an increase in the relative proportion of channel openings to the higher conductance levels without changing the amplitude of conductance levels (Derkach et al., 1999; Kristensen et al., 2011; Jenkins and Traynelis, 2012). By contrast, it is unknown whether phosphorylation of either Ser818 or Thr840 can directly regulate the function of the GluA1 AMPA receptor.

Here, we show that PKC increases conductance of native AMPA receptors in hippocampal neurons independent of actions at GluA1-Ser831, likely via phosphorylation of GluA1-Ser818 and -Thr840. We identify the functional effects of phosphomimetic mutations at GluA1-Ser818 and -Thr840 and the structural determinants within the GluA1 C-terminus that mediate the phosphorylation-induced changes in conductance. Our NMR and modeling data suggest that a highly ordered structure exists in the C-terminal domain at these sites that change in response to phosphorylation. These findings provide new insight into the structural changes induced by phosphorylation of the GluA1 AMPA receptor subunit, which are critical during synaptic plasticity.

Materials and Methods

Molecular biology

Molecular Pharmacology Fast Forward. Published on January 22, 2014 as DOI: 10.1124/mol.113.091488
This article has not been copyedited and formatted. The final version may differ from this version.

The coding region of rat *GRIA1* gene (within the CMV-based mammalian expression vector pRK5, BD Pharmingen, San Diego, CA. USA) was used for transient expression of GluA1 (GenBank accession # M38060.1). All mutations were inserted into GluA1 constructs using the QuikChange mutagenesis method according to the Stratagene protocol; cDNA sequences were verified by DNA sequencing (Operon, Huntsville, AL. USA).

Maintenance and transfection of HEK cells

All cell biology reagents were from Gibco (Invitrogen, Grand Island, NY. USA) unless otherwise stated. Human embryonic kidney 293 cells (HEK, ATCC CRL-1573) were maintained in GlutaMAX Dulbecco's modified Eagle's medium (DMEM) supplemented with 10% (v/v) fetal calf serum, 100 units/ml of penicillin, and 10 µg/ml of streptomycin. Cells were grown on polystyrene culture dishes or 8 mm glass coverslips coated with 0.05 mg/ml poly-D-lysine (Millipore, Billerica, MA. USA) contained in 24-well tissue culture plates, and incubated in 5% CO_2, 95% O_2 at 37°C. Trypsin-EDTA (0.05%) was used to passage cells. Cells plated on coverslips were transfected using FuGene6 or X-tremeGene9 (Roche, Nutley, NJ. USA) according to the manufacturer's protocol. After transfection, HEK cells were grown in DMEM supplemented with 200 µM NBQX (2,3-dihydroxy-6-nitro-7-sulfamoyl-benzo[f]quinoxaline-2,3-dione, an AMPA receptor antagonist; Tocris, Minneapolis, MN) to protect against excitotoxicity.

Recording of macroscopic currents from excised membrane patches

Outside-out membrane patches were excised from transiently transfected HEK cells using fire polished borosilicate micropipettes with a tip resistance of 4-6 MΩ. The internal

Molecular Pharmacology Fast Forward. Published on January 22, 2014 as DOI: 10.1124/mol.113.091488
This article has not been copyedited and formatted. The final version may differ from this version.

solution was comprised of (in mM) 110 gluconic acid, 110 CsOH, 30 CsCl, 4 NaCl, 5 HEPES, 4.37 EGTA, 2.1 $CaCl_2$, 2.27 $MgCl_2$, 0.1 spermine (Sigma-Aldrich, St. Louis, MO. USA), 4 ATP, 0.3 GTP. The pH was adjusted to 7.3 with CsOH. For some experiments, the internal solution was supplemented with 20 nM Protein Kinase C catalytic subunit (Sigma Aldrich, St. Louis, MO. USA). External recording solution for all experiments was comprised of (in mM) 150 NaCl, 10 HEPES, 3 KCl, 1 $CaCl_2$, 1 $MgCl_2$, pH 7.4; 310-330 mOsm. Currents were recorded at room temperature (23^{o}C) at a holding potential (V_{HOLD}) of -60 mV using a HEKA EPC9 amplifier, filtered at 5 kHz (-3dB), and digitized at 20 kHz. ChanneLab (Synaptosoft, Decatur, GA. USA) was used to perform stationary variance analysis of macroscopic currents, as previously described (Traynelis and Jaramillo, 1998; Jin et al., 2003; Kristensen et al., 2011). Briefly, the current response during agonist washout was divided into 100 portions that showed on average an equal decrement of the current. The variance was calculated for all data points in each section, and baseline variance subtracted from this. Variance (σ^2) can be related to the macroscopic (I) and unitary current (i) amplitude by

$$\sigma^2 = i I - (I^2 / N) \qquad (1)$$

where N is the number of channels. Non-linear least squares fitting of this equation to the data was used to determine the unitary current, number of channels and open probability (P_O). The unitary current is a weighted mean average of all single channel conductance levels (Cull-Candy et al., 1988; Traynelis and Jaramillo, 1998).

For measurement of rapidly desensitizing current responses, a piezoelectric crystal-driven double-barreled perfusion system was used to rapidly apply saturating concentrations of agonist onto excised membrane patches for 100-200 ms, as previously described (Traynelis and Wahl, 1997). The time course of solution exchange across the laminar flow

Molecular Pharmacology Fast Forward. Published on January 22, 2014 as DOI: 10.1124/mol.113.091488
This article has not been copyedited and formatted. The final version may differ from this version.

interface was estimated by the 10-90% rise time (0.1-0.4 ms) for the open tip liquid junction potential change in response to solution of different ionic strength. Response time courses were fitte with:

$$\text{Response} = Amp_{\text{FAST}} \exp(-\text{time} / \tau_{FAST}) + Amp_{\text{SLOW}} \exp(-\text{time} / \tau_{SLOW}) \qquad (2)$$

where τ_{FAST} is the fast time constant, τ_{SLOW} is the slow time constant, Amp_{FAST} is the amplitude of the fast component, and Amp_{SLOW} is the amplitude of the slow component.

The glutamate concentration-response relationship in mutant GluA1 receptors was determined using whole-cell voltage clamp recordings at room temperature (22-25°C). Recordings were performed 24-48 hours after transfection. Two 10-channel infusion pumps (KD Scientific, Holliston, MA) and a rapid solution exchanger (RSC160, Bio-Logic, Claix, France) were used to apply agonist dissolved in extracellular solution at a rate of 1 ml/min. Whole cell patch clamp recordings on transfected HEK cells, held at -60 mV, were performed with a MultiClamp 700B amplifier and Digi-Data 1322A interface (Molecular Devices, Sunnyvale, CA) filtered at 5 kHz and digitized at 20kHz. Increasing concentrations of glutamate (8 total) were applied to four or five cells for each mutant receptor. Analysis of recordings was carried out using MatLab (The Math Works, Inc. Natick, MA). Peak currents (I) were fitted with the Hill equation:

$$I = \frac{I_{\max} * [\text{Glutamate}]^{nH}}{[\text{Glutamate}]^{nH} + EC_{50}^{nH}} \qquad (3)$$

Biochemical analysis of GluA1 phosphorylation

Molecular Pharmacology Fast Forward. Published on January 22, 2014 as DOI: 10.1124/mol.113.091488
This article has not been copyedited and formatted. The final version may differ from this version.

A construct consisting of the GluA1 C-terminus (80 amino acids) fused to a *myc* epitope tag was transfected into HEK cells with either prK5 empty vector or PKCα. 36 h post-transfection cells were stimulated for 5 min with 1 μM PMA. Cells were briefly rinsed in ice-cold phosphate-buffered saline and lysed in buffer comprised of 25 mM Tris pH7.4, 1.0% Triton-X-100, 0.5% sodium deoxycholate, 0.1% sodium dodecyl sulfate, 100 mM NaCl, 50 mM NaF, 10 mM sodium pyrophosphate, 2 mM EDTA, 2 mM EGTA and supplemented with protease inhibitors (Complete Protease Cocktail, Roche). The GluA1 C-terminus was immunoprecipitated using *myc* ascites (generated in house) and Protein A beads (GE Healthcare). Proteins were eluted with SDS-loading sample buffer and heated to 65°C for 10 min then run through SDS-PAGE and transferred to polyvinylidene fluoride membranes (Millipore) for western blotting, as previously described (Boehm et al., 2006b; Lee et al., 2007). Antibodies used for western blot analysis were as follows: PKCα (1:1000, BD transduction labs); GAPDH (1:20,000, Sigma); phosphoserine-831 (1:4000, Millipore). Antibodies generated in house: phosphoserine-818 (1:250, JH5888); phosphothreonine-840 (1:500, JH2871); GluA1 (1:2000, JH4294) (Boehm et al., 2006b; Lee et al., 2007).

Preparation of primary cultures of hippocampal neurons

All procedures involving the use of animals were reviewed and approved by the Emory University Institutional Animal Care and Use Committee. The hippocampus was dissected from the brains of both male and female P0 129X1/Svj GluA1-S831A knock-in mice (Lee et al., 2010). Tissue was incubated in a dissociation medium comprised of (in mM) 82 Na_2SO_4, 30 K_2SO_4, 5.8 $MgCl_2$, 0.25 $CaCl_2$, 1 HEPES, 3.6% glucose, 0.1 kynurenic acid, and phenol red, pH 7.4 with NaOH. Hippocampal tissue was incubated in papain (20 mg/ml, Worthington

Molecular Pharmacology Fast Forward. Published on January 22, 2014 as DOI: 10.1124/mol.113.091488
This article has not been copyedited and formatted. The final version may differ from this version.

Biochemical, cat #LS003124, Lakewood, NJ) to digest for 15 minutes then transferred to a 30 mg/ml ovomucoid trypsin inhibitor solution (Sigma-Aldrich, cat #T92531) for an additional 15 minutes. The tissue was then triturated using two Pasteur pipettes of varying bore sizes in OPTI-MEM (Life technologies) supplemented with 2.5% glucose. Cells were diluted to a concentration of 0.2 x 10^6 cells/ml and 1 ml was plated onto 50 mg/ml poly-D-lysine-coated glass coverslips (diameter 8 mm) in 24 well plates. After cells settled and stuck to coverslips, OPTI-MEM was exchanged for Neurobasal medium supplemented with 1 ml 100X Glutamax/500 ml of medium, 10 ml 50X B-27 supplement/500 ml medium (Gibco cat # 17504-044), and 5 ml of 10,000 U/ml penicillin and 10,000 μg/ml of streptomycin per 500 ml of medium. Cells were cultured for 7 to 14 days in 95% O_2 / 5% CO_2 at 37^{o}C and media was exchanged every 3-4 days.

Molecular modeling

The GluA1 and GluA2 sequences of *Rattus norvegicus* (accession numbers P19490.2, NP_001077280) were aligned with TCoffeeWS in the Jalview sequence alignment editor (version 2.7). The output was used for constructing a multiple alignment for modeling of the GluA1 tetramer based on the crystal structure of the GluA2 tetramer (pdb id: 3KG2, 63% identity/75% similarity for the aligned length as used for modeling). Homology models were built using Modeller 9.11 using the very slow refinement setting while applying α-helical restraints to residues 810-819 and 825-838 in each chain.

NMR spectroscopy and structural calculations

Molecular Pharmacology Fast Forward. Published on January 22, 2014 as DOI: 10.1124/mol.113.091488
This article has not been copyedited and formatted. The final version may differ from this version.

All experiments were performed on a Varian Inova 500 Spectrometer with a triple resonance gradient probe at the Cornell Biomolecular NMR Center. Homonuclear 2D NOESY, TOCSY, ROESY, and COSY, spectra were obtained at 1˚C, 5˚C, 15˚C, and 25˚C. A DIPSI-2 (Rucker and Shaka, 1989) sequence of 80 ms was used in the TOCSY experiments, a 150 ms mixing period was used in the NOESY experiments, and 250 ms in the ROESY experiments. 2D [^{1}H,^{15}N]HSQC and [^{1}H,^{13}C]HSQC spectra were acquired with natural abundance proteins. Data were processed either with NMRPipe, (Delaglio et al., 1995) Sparky (Goddard and Kneller) was used for data visualization, assignments, and peak integration.

Distance constraints for structural calculations were obtained from 2D homonuclear NOESY experiments at 1˚C in 90% H_2O/10% D_2O, and were classified into four categories according to the intensity of the NOE crosspeak (<2.5, <3.0, and <4.0 Å). The distance restraints and chemical shifts (Cα, Cβ, and Hα) were used as inputs to determine structures using the simulated annealing protocol in XPLOR-NIH (Schwieters et al., 2006). The structures were visualized using Pymol (Schrödinger, NY, NY) and analyzed using Procheck-NMR and Aqua (Laskowski et al., 1996). The Ramachandran statistics for the unphosphorylated peptide were 47.1% most favored, 35.3% additional allowed, 11.8% generously allowed, 5.9% disallowed; and those for the phosphorylated peptide were 29.4% most favored, 58.8% additional allowed, 11.8% generously allowed.

Statistical methods.

Results are expressed as mean ± SEM. Statistical analysis of pairwise or multiple comparisons were performed using Student's *t*-test or ANOVA with Tukey's post hoc test. $p <$

Molecular Pharmacology Fast Forward. Published on January 22, 2014 as DOI: 10.1124/mol.113.091488
This article has not been copyedited and formatted. The final version may differ from this version.

0.05 was considered to be statistically significant. Power of all statistical tests was at least 0.8. The number of patches for all experiments is reported as (n).

Results

PKC increases conductance of hippocampal AMPA receptors

Phosphorylation of GluA1 Ser831 by CaMKII has previously been shown to increase the frequency of channel openings to higher conductance levels (Derkach et al., 1999; Derkach, 2003; Kristensen et al., 2011). In contrast, the functional effects of GluA1 phosphorylation by PKC (Tavalin, 2008) have received less attention. Recently, we have shown that purified PKC, like CaMKII, phosphorylates GluA1 Ser831 to increase AMPA receptor conductance (Jenkins and Traynelis, 2012). However, whether PKC alters neuronal AMPA receptor function through phosphorylation of residues other than GluA1 Ser831 has not been fully explored. To better understand the functional effects of PKC, we first determined whether PKC can increase native AMPA receptor conductance in hippocampal neurons. Cultured neurons were isolated from GluA1-S831A knock-in mice in order to prevent phosphorylation of GluA1 Ser831 by PKC. Use of this mutant mouse should allow us to determine whether PKC can enhance AMPA receptor conductance via actions at residues other than GluA1 Ser831. Macroscopic outside-out patches were excised from cultured GluA1-S831A hippocampal pyramidal neurons and recordings were performed in the presence of DL-APV (100 μM) and Mg^{2+} (1 mM) to block NMDA receptors and isolate AMPA receptor current. External solutions were further supplemented with cyclothiazide (100 μM) to minimize AMPA receptor desensitization and yield a current response with a slow washout period following 1 mM glutamate application (Figure 1A). We have previously described the

Molecular Pharmacology Fast Forward. Published on January 22, 2014 as DOI: 10.1124/mol.113.091488
This article has not been copyedited and formatted. The final version may differ from this version.

current-voltage relationship for these neuronal responses as linear (Kristensen et al., 2011), suggesting native AMPA receptors in our cultured hippocampal neurons contain both GluA1 and edited GluA2. The weighted mean conductance (γ_{MEAN}) of the AMPA receptors expressed in the outside-out patch was estimated using variance analysis of the graded macroscopic current response during slow channel deactivation (Traynelis and Jaramillo, 1998; Jin et al., 2003; Kristensen et al., 2011) (Figure 1B). Including the purified catalytic subunit of PKC (20 nM) in the patch pipette solution significantly increased the γ_{MEAN} of hippocampal neuronal AMPA receptors (Figure 1C) from 5.4 pS ± 0.6 (n=11) in control recordings lacking PKC to 9.8 ± 1.3 pS (n=9, $p<0.01$ Student's *t*-test, Figure 1D). These data are consistent with a PKC-induced increase in native AMPA receptor function by means other than phosphorylation of GluA1 Ser831.

Phosphorylation of GluA1-Ser818, Ser831 and Thr840 increase conductance

Because hippocampal pyramidal neurons express a heterogeneous population of AMPA receptors that include receptors containing GluA1 (Sommer et al., 1990; Wenthold et al., 1996; Lu et al., 2009), we examined whether PKC exerts its effects on AMPA receptor function via known PKC phosphorylation targets within the GluA1 C-terminus (Roche et al., 1996; Boehm et al., 2006b; Lee et al., 2007; Lin et al., 2009). We first evaluated whether PKC can phosphorylate each site using a truncated GluA1 C-terminus construct expressed in HEK cells and phospho-specific antibodies towards Ser818, Ser831, and Thr840. The GluA1 C-terminal domain fused to a *myc* epitope tag was transfected into HEK cells with and without PKC. PKC was activated with PMA, and lysates were collected and proteins eluted and run through SDS polyacrylamide gel electrophoresis Phospho-specific antibodies were

Molecular Pharmacology Fast Forward. Published on January 22, 2014 as DOI: 10.1124/mol.113.091488
This article has not been copyedited and formatted. The final version may differ from this version.

used in a western blot analysis to identify whether PKC enhanced phosphorylation at either GluA1 Ser818, Ser831 and Thr840. Figure 1E summarizes data confirming that co-expression of active PKC can increase the phosphorylation at each of these sites.

We subsequently recorded the response properties under voltage clamp of homomeric GluA1 receptors transiently expressed in HEK cells. GluA1 cDNAs were subjected to mutagenesis to alter four residues that are known substrates for phosphorylation. This approach has previously been shown to reproduce the conductance changes produced by phosphorylation of Ser831 (Derkach et al., 1999; Kristensen et al., 2011). We inserted phosphodeficient (alanine) or phosphomimetic (glutamate) mutations at GluA1 Ser818, Ser831, and Thr840. In addition, we placed a phosphodeficient alanine mutation at GluA1 Ser845, a residue that is phosphorylated by PKA (Banke et al., 2000) to minimize potential effects of endogenous phosphorylation at this site, which might have biased our results. All constructs also included the GluA1-L497Y (GluA1-LY) mutation to block AMPA receptor desensitization (Stern-Bach et al., 1998) in order to perform variance analysis. Mutant GluA1 receptors were transfected into HEK cells, from which outside-out patches were excised. The variance of the current response to 1 mM glutamate was subsequently evaluated. When a phosphomimetic glutamate substitution was made at GluA1 Ser818 together with phosphodeficient alanine substitutions at GluA1 Ser831, Thr840 and Ser845 (GluA1-LY-EAAA), conductance was significantly increased compared to a GluA1 construct in which all four residues are mutated to alanine (GluA1-LY-AAAA, Table 1). GluA1-LY-AAAA receptors were used as controls for these experiments in order to compare phosphomimetic receptors to a receptor completely devoid of phosphorylation at the residues of interest. Similarly, when GluA1 Thr840 was mutated to glutamate with alanine substitutions at the other 3

Molecular Pharmacology Fast Forward. Published on January 22, 2014 as DOI: 10.1124/mol.113.091488
This article has not been copyedited and formatted. The final version may differ from this version.

residues (GluA1-LY-AAEA) or when GluA1 Ser831 was mutated to glutamate with alanines at the other 3 residues (GluA1-LY-AEAA), conductance was increased compared to the GluA1-LY-AAAA control (Table 1). Phosphomimetic mutations at Ser818, Ser831, or Thr840 did not alter open probability (P_O) of the GluA1-LY mutant (Table 1), but a phosphomimetic mutation at GluA1-Ser845 significantly enhanced P_O compared to GluA1-LY-AAAA receptors ($p<0.05$, Student's *t*-test), as described previously (Banke et al., 2000).

To examine whether there are additive or synergistic effects of simultaneous phosphorylation at multiple sites, we mutated pairs of 2 residues to glutamate while the others were changed to alanine. We performed variance analysis on currents elicited from transfected HEK cell patches. When glutamate substitutions were made at both GluA1 Ser818 and Ser831 (GluA1-LY-EEAA), at both GluA1 Ser818 and Thr840 (GluA1-LY-EAEA) or at both GluA1 Ser831 and Thr840 (GluA1-LY-AEEA), γ_{MEAN} was not significantly changed compared to receptors in which a single glutamate substitution was made ($p>0.05$ for all comparisons by one-way ANOVA; Table 1). Statistical comparisons were made between constructs in which a single phosphomimetic residue was inserted at Ser818, Ser831, or Thr840 and those constructs in which the same residue was mutated to glutamate in addition to one other residue. There was no significant difference between GluA1-EAAA, GluA1-EEAA and GluA1-EAEA (by ANOVA, $p>0.05$). GluA1-AEAA was not significantly different from GluA1-EEAA and GluA1-AEEA (by ANOVA, $p>0.05$). There was also no difference between GluA1-AAEA, GluA1-EAEA and GluA1-AEEA (by ANOVA, $p>0.05$). In addition, there was no significant difference between GluA1-AAAA and GluA1-EEEA (by ANOVA, $p>0.05$; Table 1). These data suggest that a single phosphorylation event within the GluA1 C-terminus is sufficient to increase conductance to its apparent maximal level.

Molecular Pharmacology Fast Forward. Published on January 22, 2014 as DOI: 10.1124/mol.113.091488
This article has not been copyedited and formatted. The final version may differ from this version.

Phosphomimetic GluA1 mutations do not alter response time course or agonist potency

We subsequently evaluated whether phosphomimetic mutations at these PKC phosphorylation sites altered other aspects of channel function. We examined glutamate concentration-response relationships for each phosphomimetic mutation in whole-cell patch clamp experiments using transfected HEK cells (Figure 2A-C). Parameters that define the glutamate concentration-effect relationship were not significantly different in the GluA1-LY-EAAA, GluA1-LY-AEAA, or GluA1-LY-AAEA receptors compared to control GluA1-LY-AAAA receptors ($p>0.05$ by one-way ANOVA; Figure 2B,C, Table 1). In addition, the concentration-effect relationships of all phosphomimetic and phosphodeficient mutant receptors were unchanged compared to GluA1-L497Y receptors with a wild-type C-terminus. These data establish that glutamate EC_{50} was unaffected by any of the phosphomimetic mutations inserted at GluA1 Ser818, Ser831 or Thr840.

We subsequently examined whether GluA1 response time course was altered by phosphomimetic mutations at each PKC phosphorylation site (GluA1-EAAA, AEAA, AAEA). To do this, we used a rapid perfusion system with an open tip solution exchange time of 0.1-0.4 ms to apply a maximally effective concentration (10 mM) of glutamate to outside-out patches excised from transiently transfected HEK cells. We measured deactivation time course following rapid glutamate removal in GluA1-L497Y phosphomimetic mutant receptors (Figure 2D,E). Neither the 10-90% rise time, the time constants describing deactivation, τ_{fast} ($\tau_{f\text{-}deact}$) and τ_{slow} ($\tau_{s\text{-}deact}$), nor the steady-state to peak ratio (SS/PK) were significantly different among the phosphomutant GluA1 receptors (Table 2). We also examined rates of desensitization in phosphomutant receptors in which GluA1 Leu497 was not mutated

Molecular Pharmacology Fast Forward. Published on January 22, 2014 as DOI: 10.1124/mol.113.091488
This article has not been copyedited and formatted. The final version may differ from this version.

(Figure 2E), which allowed desensitization to proceed. Again, neither 10-90% rise time, time constants describing desensitization ($\tau_{f\text{-}desens}$, $\tau_{s\text{-}desens}$) nor the SS/PK ratio were significantly different in GluA1-EAAA, GluA1-AEAA or GluA1-AAEA receptors compared to GluA1-AAAA control receptors ($p>0.05$ by one-way ANOVA; Table 2). Taken together, these data suggest that the primary effects of phosphomimetic mutations at GluA1 Ser818, Ser831 and Thr840 are on single channel conductance in homomeric GluA1 receptors.

Structural specificity of the GluA1 phosphorylation-mediated conductance increase

Because phosphorylation at three different sites within a relatively short region of GluA1 C-terminus can all increase conductance, we tested whether phosphomimetic mutations at additional nearby sites within this region could also increase GluA1 conductance. We substituted a glutamate at each residue in the GluA1 membrane proximal C-terminus with glutamate up until GluA1-Thr840 using site-directed mutagenesis. Residues GluA1-Glu809 to Lys812 were not tested in this experiment because glutamate substitutions at those sites significantly reduced response amplitude, which may reflect reduced surface expression (Boehm et al., 2006b). Outside-out patches were excised from HEK cells transfected with the mutant receptors, and experiments were carried out in groups of 3 consecutive phosphomimetic receptors with the phosphodeficient control (GluA1-LY-AAAA) on the same recording days; statistical comparisons were made within each of these groups of four mutant receptors (Figure 3A). We applied variance analysis to the non-desensitizing currents to estimate γ_{MEAN}. We found that only the GluA1-S818E, -S831E and -T840E mutations significantly increased conductance compared to GluA1-LY-AAAA control receptors (Figure 3A; $p<0.01$ by one-way ANOVA with Tukey's post-hoc test). That is, conductance is

Molecular Pharmacology Fast Forward. Published on January 22, 2014 as DOI: 10.1124/mol.113.091488
This article has not been copyedited and formatted. The final version may differ from this version.

unaffected by phosphomimetic mutations at all other residues, including those immediately adjacent to these three sites ($p>0.05$ for all comparisons by one-way ANOVA; Figure 3A). These data suggest that GluA1 Ser818, Ser831 and Thr840 are uniquely positioned within the C-terminal domain to induce the specific conformational changes necessary to increase conductance upon addition of a phosphate molecule by PKC. That is, the data suggest a tightly controlled structure involving this region of the C-terminal domain.

The structural determinants for regulation of AMPA receptor conductance

There is currently no structural or functional information about the configuration of the GluA1 C-terminus. Moreover, according to the Phyre2 structure prediction model, this sequence shares minimal homology with any proteins for which structural data is available (Kelley and Sternberg, 2009). Thus, the manner by which residues in the C-terminus impact gating remains largely speculative. To investigate the structural determinants within the C-terminal domain that underlie the phospho-dependent GluA1 conductance increase, we deleted increasing portions of the distal C-terminus from the GluA1-LY-S831E phosphomimetic receptor. Outside-out patches were excised from the HEK cells and non-desensitizing GluA1 truncation mutant receptor currents elicited in response to a maximally effective glutamate concentration were assessed with variance analysis to estimate changes in γ_{MEAN}. The initial hypothesis was that a PDZ protein (post-synaptic density-95, discs-large, zona occludens 1 protein) binds to the distal GluA1 C-terminus to induce a conformational change in channel structure associated with the phosphorylation-dependent increase in γ_{MEAN}. If this is true, then removing the GluA1 PDZ binding-domain by inserting a stop codon at GluA1-Ala886 should abrogate the effects of the GluA1-S831E mutation. However, the

Molecular Pharmacology Fast Forward. Published on January 22, 2014 as DOI: 10.1124/mol.113.091488
This article has not been copyedited and formatted. The final version may differ from this version.

S831E mutation still induced an increase in conductance of GluA1 receptors lacking a PDZ binding-domain (GluA1-S831E-Δ886; 13.5 ± 0.9 pS) compared to phosphodeficient full-length receptors (9.7 ± 0.7 pS; Figure 3B,C; $p<0.05$, one-way ANOVA, Tukey's post-hoc test). Inserting stop codons at incremental intervals upstream of the PDZ-binding region of GluA1 failed to interrupt the increase in γ_{MEAN} compared to full-length phosphodeficient receptors (Figure 3B,C; $p<0.05$, one-way ANOVA, Tukey's post hoc test). However, stop codons inserted upstream of Ser850 at Ser845 (10.2 ± 0.9 pS), Thr840 (9.6 ± 0.7 pS) and Ser836 (9.3 ± 0.9 pS) prevented the phosphomimetic GluA1-S831E-mediated increase in conductance compared to full-length phosphodeficient receptors (9.7 ± 0.7 pS; $p=1.0$, one-way ANOVA, Tukey's post hoc test). This finding suggests that residues within the membrane proximal C-terminal domain, upstream of Ser850, are required to induce the conformational changes necessary for the phospho-Ser831-dependent conductance increase. To evaluate this idea further, we inserted stop codons at residues 846, 847, 848, and 849, each of which blocked the increase in conductance caused by the phosphomimetic GluA1-S831E mutation. From these data we have identified two critical regions within the C-terminal domain, "C1," comprised of the membrane proximal region, and "C2," the more distal C-terminal domain, which are separated by a glycine-rich 6 residue flexible linker.

To determine if GluA1 Ser818 and Thr840 require similar regions of the C-terminal domain and thereby likely possess similar structural determinants of the phospho-mediated conductance increase, stop codons were inserted before and after the critical Ser845-GAGA-Ser850 region in the GluA1-LY-EAAA and GluA1-LY-AAEA mutant receptors. If phospho-Ser818 and phospho-Thr840 possess the same structural determinants for increasing GluA1 conductance as phospho-Ser831, then a stop codon inserted at GluA1 Gly846 (but not

Molecular Pharmacology Fast Forward. Published on January 22, 2014 as DOI: 10.1124/mol.113.091488
This article has not been copyedited and formatted. The final version may differ from this version.

Ser850) should block the phosphomimetic-mediated conductance increase. Currents from outside-out patches excised from HEK cells transiently transfected with these mutant GluA1 receptors were evaluated for changes in γ_{MEAN} using variance analysis. The increase in conductance by the Thr840 phosphomimetic mutation in GluA1-LY-AAEA receptors was blocked by a stop codon inserted at GluA1 Ser846 but not by a GluA1 Ser850 stop codon (Table 3). By contrast, the conductance increase in GluA1-LY-EAAA receptors was blocked by stop codons inserted at both GluA1 Gly846 and Ser850 (Table 3). Together, these data suggest that GluA1 Ser831 and Thr840 possess similar structural determinants controlling the phospho-dependent conductance increase, while GluA1 Ser818 requires a greater length of the GluA1 C-terminus to induce the same changes in receptor function.

GluA1 C-terminal structure

The Phyre2 protein homology/analogy recognition engine predicts that residues forming the membrane proximal region of the GluA1 C-terminus consists of two helices separated by residues GluA1 Cys825 to Pro828 which form an unstructured linker (Kelley and Sternberg, 2009). The first helix is predicted to extend the M4 helix that spans the membrane. In addition, Phyre2 disorder prediction models indicate that the residues forming the glycine-rich region are likely disordered, supporting the hypothesis that this also forms a flexible linker. In light of these findings, a model of the GluA1 C-terminus was developed (Figure 4AB). Homology models were built by applying alpha-helical restraints to residues 810-819 and 825-838 in each chain, based on medium- to high-confidence secondary structure predictions with the Phyre2 algorithm**.** The tetrameric antagonist-bound GluA2 crystal structure (Sobolevsky et al., 2009) was used to illustrate the extracellular and

Molecular Pharmacology Fast Forward. Published on January 22, 2014 as DOI: 10.1124/mol.113.091488
This article has not been copyedited and formatted. The final version may differ from this version.

membrane-bound regions of the GluA1 receptor, shown in grey. Shown on the intracellular side of a single subunit is our molecular model of the predicted structure of the C-terminal domain. The "C1" region is comprised of two helices. The more membrane proximal helix, containing GluA1 Ser818, extends the M4 helix into the cytoplasm, whereas GluA1 Ser831 and Thr840 bracket the second helix (residues highlighted in blue spheres). This structural prediction fits with the observation that Ser818 has different structural determinants of phospho-dependent conductance changes than do Ser831 and Thr840. The C_α positions of the critical G-A-G-A residues required for the phospho-Ser831 and phospho-Thr840 mediated conductance increase are highlighted in yellow (1.2 × van Der Waals radii).

We subsequently utilized NMR spectroscopy to assess the secondary and tertiary structure of this region of the GluA1 C-terminus predicted by molecular modeling to be helical (refinement statistics are contained in Table 4). A peptide sequence consisting of GluA1 residues 828-849 (PQQSINEAIRTSTLPRNSGAGA), which includes the predicted second helix, provided interpretable data in solution using NMR spectroscopy. We analyzed peptides that were phosphorylated and unphosphorylated at Ser831 and Ser845. The [^{1}H,^{15}N]HSQC spectra of the wild-type peptide as well as the phosphorylated Ser831 and Ser845 forms were well-dispersed, allowing assignments using standard homonuclear methods. The Chemical Shift Index did not predict secondary structure for any of the peptides, although chemical shift changes with Ser831 phosphorylation in the first half of the peptide were consistent with an increase in helical propensity (decreased Cα and increased Hα chemical shift; Figure 4C, Figure 5). The rotating-frame nuclear Overhauser effect correlation spectra (ROESY) for the two phosphorylated peptides showed exchange peaks of amide protons with bulk water only in the second half of the peptide, whereas wild type unphosphorylated

Molecular Pharmacology Fast Forward. Published on January 22, 2014 as DOI: 10.1124/mol.113.091488
This article has not been copyedited and formatted. The final version may differ from this version.

peptide showed exchange only in the second residue (Gln829). Phosphorylation of Ser831 resulted in long-range chemical shift changes, perhaps consistent with a defined structure. By contrast, phosphorylation of Ser845 resulted in only local chemical shift changes (Figure 4C, Figure 5).

The chemical shift and ROESY spectra suggest the possibility of transient secondary structure. Cooling the sample to 1˚C decreased rotational correlation time sufficiently to obtain excellent nuclear Overhauser effect spectra (NOESY). Using distance constraints from the NOESY experiment, structures were determined for the wild type and phosphorylated Ser831 peptides. As the peptide may exist in both unfolded and partially helical forms, the chemical shift values are a weighted average of all conformations and the NOE constraints reflect only those conformations in which the distances between two protons are less than approximately 5 Å. Thus, the ensemble of structures is weighted toward those for which some regular secondary structure is present. As shown in Figure 4, the first half of the peptide (Ile832 to Arg837) is consistent with an α-helix (presumably a transient helix), corresponding to part of the second C1 helix predicted by the modeling. Modeling studies suggest that the G-A-G-A residues could fold back on the second C1 helix. Although the truncated peptide is too flexible to determine this definitively, phosphorylation of Ser831 does result in significant chemical shift changes throughout the first half of the peptide. In contrast, phosphorylation of Ser845 results in only local chemical shift changes.

Discussion

Physiological significance of GluA1 phosphorylation by PKC

Molecular Pharmacology Fast Forward. Published on January 22, 2014 as DOI: 10.1124/mol.113.091488
This article has not been copyedited and formatted. The final version may differ from this version.

Phosphorylation-mediated conductance changes in GluA1 AMPA receptors have long been hypothesized to be an important step in the expression of synaptic plasticity and LTP (Barria et al., 1997b; Benke et al., 1998; Poncer et al., 2002; Esteban et al., 2003; Lee et al., 2003; Luthi et al., 2004; Lee et al., 2007; Lin et al., 2009; Lee et al., 2010; Makino et al., 2011). Our results establish two novel sites (Ser818 and Thr840) by which PKC can enhance AMPA receptor conductance in hippocampal AMPA receptors. Previous work indicates that PKC phosphorylation of GluA1 Ser818 is critical for LTP and promotes synaptic incorporation of GluA1 subunits (Boehm et al., 2006b; Lin et al., 2009). Additional work has suggested a specific mechanism by which these actions occur where phosphorylation at Ser818 facilitates binding of GluA1 to the actin-binding protein 4.1N, thereby enhancing activity-dependent insertion of GluA1 into extrasynaptic pools. Extrasynaptic AMPA subunits can be delivered to the synapse during synaptic potentiation and LTP. Replenishing this supply via phosphorylation at GluA1-Ser818 facilitates LTP expression (Lin et al., 2009). A similar interaction occurs between 4.1N and kainate receptors. However, PKC activation inhibits the interaction of kainate receptors with 4.1N (Copits and Swanson, 2013). Phosphorylation by PKC could therefore have simultaneous opposing actions on kainate and AMPA receptors, which may be critical during synaptic scaling. In conjunction with these previous studies, our findings suggest that the impact of GluA1 Ser818 phosphorylation by PKC is two-fold; not only is there a greater supply of extrasynaptic AMPA receptors for synaptic delivery after Ser818 phosphorylation, but upon delivery, the newly inserted receptors have greater single channel conductance. With this in mind, it seems likely that phosphorylation at this residue could have an even greater impact on AMPA receptor synaptic transmission and synaptic plasticity than GluA1 Ser831.

Molecular Pharmacology Fast Forward. Published on January 22, 2014 as DOI: 10.1124/mol.113.091488
This article has not been copyedited and formatted. The final version may differ from this version.

While less is known about the functional consequences of GluA1 Thr840 phosphorylation, it may play a role in expression of adult-forms of LTP (Lee et al., 2007). Other studies suggest that GluA1 Thr840 is not phosphorylated by PKC but rather by p70S6 kinase, and a decrease in GluA1 Thr840 phosphorylation is triggered by induction of LTD (Delgado et al., 2007). Despite these inconsistent findings, our data suggest that addition of a phosphate group to GluA1 Thr840 would increase AMPA receptor conductance and overall charge transfer. Our findings may help to explain the mechanism by which phosphoThr840 regulates synaptic plasticity. Moreover, our findings further suggest that multiple signaling cascades that induce CaMKII-, PKC-, or p70S6 kinase-mediated phosphorylation of GluA1 receptors converge on a single functional consequence (an increased single channel conductance) within a small region (Ser818-Thr840). The finding that multiple signaling cascades achieve a single functional outcome, harnessing control of GluA1 conductance via the C-terminus, underscores the importance of AMPA receptor conductance in synaptic transmission and plasticity.

Structural determinants of the phosphorylation-induced increase in GluA1 conductance

Virtually no structural information exists for the AMPA receptor C-terminal domain, and it remains unknown how the C-terminal domain interacts with itself or other parts of the channel. Moreover, it is unclear if the C-terminus contains secondary structural motifs that assemble into unique tertiary structural elements, or whether it acts primarily as a flexible loop allowing scaffold proteins to bind directly to the polypeptide chain. Our data show that phosphorylation of 3 residues within a stretch of 22 residues in the GluA1 C-terminal domain increases AMPA receptor conductance, suggesting that this region of the GluA1 C-terminus

Molecular Pharmacology Fast Forward. Published on January 22, 2014 as DOI: 10.1124/mol.113.091488
This article has not been copyedited and formatted. The final version may differ from this version.

plays important structural or biophysical roles in GluA1 receptor function. Remarkably, the results of the glutamate scan show strong specificity in that phosphomimetic mutations at only these three residues increase conductance, hinting at a secondary or tertiary structure for this region that directs either specific changes in gating or interactions with function-modulating accessory/scaffolding proteins. Our molecular modeling further raises the hypothesis that two of these phosphorylation sites bracket a helix, which resides in the first of two larger domains (C1 and C2) connected by a glycine-rich flexible linker. The presence of helical forming elements is supported by our NMR data, which provides the first evidence for secondary structure within this region of the protein. The glycine-rich flexible linker may act as a hinge that allows interdomain interactions between C2 and the membrane proximal C1, which contains GluA1-Ser818. It is also noteworthy that deletion studies show similar structural requirements for Ser831/Thr840 (bracketing the helix), but a different structural requirement for Ser818 (residing in a separate predicted helix). Finally, the structural data that suggests phosphorylation at GluA1 Ser831 but not Ser845 induces chemical shift changes reflects the electrophysiological data showing that phosphorylation of GluA1 Ser831 enhances conductance whereas GluA1 Ser845 phosphorylation does not. It is likely that there are different conformational changes that follow GluA1 Ser845 phosphorylation to enhance P_O rather than conductance.

It remains unclear how phosphorylation of GluA1 Ser818 and Thr840 influences channel conductance. Previous studies have shown that phosphorylation of Ser831 increases the coupling efficiency between agonist binding to a subunit and gating (Kristensen et al., 2011). Combining this idea with data showing subunit gating contributes incrementally to conductance sublevels (Rosenmund et al., 1998) suggests that Ser831 enhances the

Molecular Pharmacology Fast Forward. Published on January 22, 2014 as DOI: 10.1124/mol.113.091488
This article has not been copyedited and formatted. The final version may differ from this version.

ability of agonist binding at each subunit to increase the probability that it will participate in gating, which increases the overall proportion of higher conductance sublevels (Derkach et al., 1999; Kristensen et al., 2011). Our working hypothesis is that the conductance change we observe following GluA1 Ser818 and Thr840 phosphorylation employs this same mechanism given the similarities in the effects as phosphorylation at Ser831. How phosphorylation of these residues could bring about an increased coupling efficiency remains unknown. We speculate that new interactions within the C-terminus appear with the addition of a phosphate group. Such interactions could change the shape of this region, raising the possibility that it either enhances or disrupts binding of an as yet unknown partner that alters gating. Alternatively, a change in the mobility of the M4-C1 helix could induce longer range intraprotein conformational changes, extending into the transmembrane gating machinery, that lead to stabilization of the open state. Elucidation of the molecular details of the effects of phosphorylation will require more extensive and detailed structural data.

Conclusion

In summary, our data not only identify new sites of action at which phosphorylation can modulate GluA1 receptor function through an increase in channel conductance, but also begin to tease apart the mechanism of action for this phenomenon. We also provide the first structural data for the GluA1 C-terminal domain in a region that constitutes a hyper-regulatory domain, which is a target for multiple kinases. The structural composition of this region could provide a new binding motif that was previously unappreciated from the linear sequence, or could also be a component of a larger set of intraprotein interactions within the C-terminal that control AMPA receptor gating.

Molecular Pharmacology Fast Forward. Published on January 22, 2014 as DOI: 10.1124/mol.113.091488
This article has not been copyedited and formatted. The final version may differ from this version.

Acknowledgements:

We thank Phuong Le, Jing Zhang, and Anel Tankovic for excellent technical support.

Authorship Contribution:

Participated in research design: M Jenkins, Wells, Bachman, Snyder, A Jenkins, Huganir, Oswald, Traynelis

Conducted experiments: M Jenkins, Bachman, Oswald

Performed data analysis: M Jenkins, Wells, Bachman, Oswald, Traynelis

Contributed to the writing of the manuscript: M Jenkins, Wells, Bachman, Snyder, A Jenkins, Huganir, Oswald, Traynelis

Molecular Pharmacology Fast Forward. Published on January 22, 2014 as DOI: 10.1124/mol.113.091488
This article has not been copyedited and formatted. The final version may differ from this version.

References

Banke TG, Bowie D, Lee H, Huganir RL, Schousboe A, Traynelis SF (2000) Control of GluR1 AMPA receptor function by cAMP-dependent protein kinase. J Neurosci 20:89-102.

Barria A, Derkach V, Soderling T (1997a) Identification of the Ca^{2+}/calmodulin-dependent protein kinase II regulatory phosphorylation site in the α-amino-3-hydroxyl-5-methyl-4-isoxazole-propionate-type glutamate receptor. J Biol Chem 272:32727-32730.

Barria A, Muller D, Derkach V, Griffith LC, Soderling TR (1997b) Regulatory phosphorylation of AMPA-type glutamate receptors by CaM-KII during long-term potentiation. Science 276:2042-2045.

Benke TA, Luthi A, Isaac JT, Collingridge GL (1998) Modulation of AMPA receptor unitary conductance by synaptic activity. Nature 393:793-797.

Bliss TV, Collingridge GL (1993) A synaptic model of memory: long-term potentiation in the hippocampus. Nature 361:31-39.

Boehm J, Ehrlich I, Hsieh H, Malinow R (2006a) Two mutations preventing PDZ-protein interactions of GluR1 have opposite effects on synaptic plasticity. Learn Mem 13:562-565.

Boehm J, Kang MG, Johnson RC, Esteban J, Huganir RL, Malinow R (2006b) Synaptic incorporation of AMPA receptors during LTP is controlled by a PKC phosphorylation site on GluR1. Neuron 51:213-225.

Kainate receptor post-translational modifications differentially regulate association with 4.1N to control activity-dependent receptor endocytosis.

Copits BA, Swanson GT (2013) Kainate receptor post-translational modifications differentially regulate association with 4.1N to control activity-dependent receptor endocytosis. J Biol Chem. 288: 8952-65.

Cull-Candy SG, Howe JR, Ogden DC (1988) Noise and single channels activated by excitatory amino acids in rat cerebellar granule nuerones. J Physiol 400: 189-222.

Delaglio F, Grzesiek S, Vuister GW, Zhu G, Pfeifer J, Bax A (1995) NMRPipe: a multidimensional spectral processing system based on UNIX pipes. Journal of biomolecular NMR 6:277-293.

Delgado JY, Coba M, Anderson CN, Thompson KR, Gray EE, Heusner CL, Martin KC, Grant SG, O'Dell TJ (2007) NMDA receptor activation dephosphorylates AMPA receptor glutamate receptor 1 subunits at threonine 840. J Neurosci 27:13210-13221.

Derkach V, Barria A, Soderling TR (1999) Ca^{2+}/calmodulin-kinase II enhances channel conductance of α-amino-3-hydroxy-5-methyl-4-isoxazolepropionate type glutamate receptors. Proc Natl Acad Sci U S A 96:3269-3274.

Derkach VA (2003) Silence analysis of AMPA receptor mutated at the CaM-kinase II phosphorylation site. Biophys J 84:1701-1708.

Esteban JA, Shi SH, Wilson C, Nuriya M, Huganir RL, Malinow R (2003) PKA phosphorylation of AMPA receptor subunits controls synaptic trafficking underlying plasticity. Nat Neurosci 6:136-143.

Goddard TD, Kneller DG SPARKY 3. In. San Francisco: University of California.

Hu GY, Hvalby O, Walaas SI, Albert KA, Skjeflo P, Andersen P, Greengard P (1987) Protein kinase C injection into hippocampal pyramidal cells elicits features of long term potentiation. Nature 328:426-429.

Jenkins MA, Traynelis SF (2012) PKC phosphorylates GluA1-Ser831 to enhance AMPA receptor conductance. Channels (Austin) 6.

Jin R, Banke TG, Mayer ML, Traynelis SF, Gouaux E (2003) Structural basis for partial agonist action at ionotropic glutamate receptors. Nat Neurosci 6:803-810.

Kelley LA, Sternberg MJ (2009) Protein structure prediction on the Web: a case study using the Phyre server. Nat Protoc 4:363-371.

Kessels HW, Malinow R (2009) Synaptic AMPA receptor plasticity and behavior. Neuron 61:340-350.

Kristensen AS, Jenkins MA, Banke TG, Schousboe A, Makino Y, Johnson RC, Huganir R, Traynelis SF (2011) Mechanism of Ca^{2+}/calmodulin-dependent kinase II regulation of AMPA receptor gating. Nat Neurosci 14:727-735.

Laskowski RA, Rullmannn JA, MacArthur MW, Kaptein R, Thornton JM (1996) AQUA and PROCHECK-NMR: programs for checking the quality of protein structures solved by NMR. Journal of biomolecular NMR 8:477-486.

Lee HK, Takamiya K, He K, Song L, Huganir RL (2010) Specific roles of AMPA receptor subunit GluR1 (GluA1) phosphorylation sites in regulating synaptic plasticity in the CA1 region of hippocampus. J Neurophysiol 103:479-489.

Lee HK, Takamiya K, Kameyama K, He K, Yu S, Rossetti L, Wilen D, Huganir RL (2007) Identification and characterization of a novel phosphorylation site on the GluR1 subunit of AMPA receptors. Mol Cell Neurosci 36:86-94.

Lee HK, Takamiya K, Han JS, Man H, Kim CH, Rumbaugh G, Yu S, Ding L, He C, Petralia RS, Wenthold RJ, Gallagher M, Huganir RL (2003) Phosphorylation of the AMPA

receptor GluR1 subunit is required for synaptic plasticity and retention of spatial memory. Cell 112:631-643.

Lee S, Song B, Kim J, Park K, Hong I, An B, Song S, Lee J, Park S, Kim J, Park D, Lee CJ, Kim K, Shin KS, Tsien RW, Choi S (2013) GluA1 phosphorylation at serine 831 in the lateral amygdala is required for fear renewal. Nat Neurosci. 16: 1436-44.

Lin DT, Huganir RL (2007) PICK1 and phosphorylation of the glutamate receptor 2 (GluR2) AMPA receptor subunit regulates GluR2 recycling after NMDA receptor-induced internalization. J Neurosci 27:13903-13908.

Lin DT, Makino Y, Sharma K, Hayashi T, Neve R, Takamiya K, Huganir RL (2009) Regulation of AMPA receptor extrasynaptic insertion by 4.1N, phosphorylation and palmitoylation. Nat Neurosci 12:879-887.

Lu W, Shi Y, Jackson AC, Bjorgan K, During MJ, Sprengel R, Seeburg PH, Nicoll RA (2009) Subunit composition of synaptic AMPA receptors revealed by a single-cell genetic approach. Neuron 62:254-268.

Luthi A, Wikstrom MA, Palmer MJ, Matthews P, Benke TA, Isaac JT, Collingridge GL (2004) Bi-directional modulation of AMPA receptor unitary conductance by synaptic activity. BMC Neurosci 5:44.

Makino Y, Johnson RC, Yu Y, Takamiya K, Huganir RL (2011) Enhanced synaptic plasticity in mice with phosphomimetic mutation of the GluA1 AMPA receptor. Proc Natl Acad Sci U S A 108:8450-8455.

Malinow R (1994) LTP: desperately seeking resolution. Science 266:1195-1196.

Malinow R, Malenka RC (2002) AMPA receptor trafficking and synaptic plasticity. Annu Rev Neurosci 25:103-126.

Mammen AL, Kameyama K, Roche KW, Huganir RL (1997) Phosphorylation of the α-amino-3-hydroxy-5-methylisoxazole4-propionic acid receptor GluR1 subunit by calcium/calmodulin-dependent kinase II. J Biol Chem 272:32528-32533.

Ouyang Y, Rosenstein A, Kreiman G, Schuman EM, Kennedy MB (1999) Tetanic stimulation leads to increased accumulation of Ca($^{2+}$)/calmodulin-dependent protein kinase II via dendritic protein synthesis in hippocampal neurons. J Neurosci 19:7823-7833.

Poncer JC, Esteban JA, Malinow R (2002) Multiple mechanisms for the potentiation of AMPA receptor-mediated transmission by α-Ca^{2+}/calmodulin-dependent protein kinase II. J Neurosci 22:4406-4411.

Poon K, Ahmed AH, Nowak LM, Oswald RE (2011) Mechanisms of modal activation of GluA3 receptors. Mol Pharmacol 80:49-59.

Prieto ML, Wollmuth LP (2010) Gating modes in AMPA receptors. J Neurosci 30:4449-4459.

Ramakers GM, Gerendasy DD, de Graan PN (1999) Substrate phosphorylation in the protein kinase Cγ knockout mouse. J Biol Chem 274:1873-1874.

Roche KW, O'Brien RJ, Mammen AL, Bernhardt J, Huganir RL (1996) Characterization of multiple phosphorylation sites on the AMPA receptor GluR1 subunit. Neuron 16:1179-1188.

Rosenmund C, Stern-Bach Y, Stevens CF (1998) The tetrameric structure of a glutamate receptor channel. Science 280:1596-1599.

Rucker SP, Shaka AJ (1989) Broadband Homonuclear Cross Polarization in 2D N.M.R. Using DIPSI-2. Mol Phys 68:509-517.

Schwieters CD, Kuszewski JJ, Marius Clore G (2006) Using Xplor–NIH for NMR molecular structure determination. Progress in nuclear magnetic resonance spectroscopy 48:47-62.

Silva AJ, Stevens CF, Tonegawa S, Wang Y (1992) Deficient hippocampal long-term potentiation in α-calcium-calmodulin kinase II mutant mice. Science 257:201-206.

Sobolevsky AI, Rosconi MP, Gouaux E (2009) X-ray structure, symmetry and mechanism of an AMPA-subtype glutamate receptor. Nature 462:745-756.

Sommer B, Keinanen K, Verdoorn TA, Wisden W, Burnashev N, Herb A, Kohler M, Takagi T, Sakmann B, Seeburg PH (1990) Flip and flop: a cell-specific functional switch in glutamate-operated channels of the CNS. Science 249:1580-1585.

Song I, Huganir RL (2002) Regulation of AMPA receptors during synaptic plasticity. Trends Neurosci 25:578-588.

Stern-Bach Y, Russo S, Neuman M, Rosenmund C (1998) A point mutation in the glutamate binding site blocks desensitization of AMPA receptors. Neuron 21:907-918.

Tavalin SJ (2008) AKAP79 selectively enhances protein kinase C regulation of GluR1 at a Ca^{2+}-calmodulin-dependent protein kinase II/protein kinase C site. J Biol Chem 283:11445-11452.

Thomas GM, Lin DT, Nuriya M, Huganir RL (2008) Rapid and bi-directional regulation of AMPA receptor phosphorylation and trafficking by JNK. EMBO J 27:361-372.

Traynelis SF, Wahl P (1997) Control of rat GluR6 glutamate receptor open probability by protein kinase A and calcineurin. J Physiol 503 (Pt 3):513-531.

Traynelis SF, Jaramillo F (1998) Getting the most out of noise in the central nervous system. Trends Neurosci 21:137-145.

Wenthold RJ, Petralia RS, Blahos J, II, Niedzielski AS (1996) Evidence for multiple AMPA receptor complexes in hippocampal CA1/CA2 neurons. J Neurosci 16:1982-1989.

Footnotes:

This work was supported by the National Instituted of Health [NS068464, NS036654, GM068935, GM073959, NS036715] and the Howard Hughes Medical Institute. The authors declare no competing financial interests.

Reprint requests should be addressed to

Stephen F. Traynelis

1510 Clifton Rd.

Department of Pharmacology, Rollins Research Center

Emory University School of Medicine

Atlanta, GA. 30322

Molecular Pharmacology Fast Forward. Published on January 22, 2014 as DOI: 10.1124/mol.113.091488
This article has not been copyedited and formatted. The final version may differ from this version.

Figure Legends

Figure 1. PKC increases conductance of neuronal AMPA receptors. ***A,*** Representative AMPA receptor current response to 1 mM glutamate in outside-out patches excised from a cultured hippocampal pyramidal neuron from 129X1/Svj GluA1-S831A knock-in mice (Lee et al., 2010). Extracellular solutions contained 100 µM cyclothiazide to block AMPA receptor desensitization, which allowed variance analysis of the response during agonist washout; 100 µM DL-APV and 1 mM Mg^{2+} were included to block NMDA receptors. The grey trace above shows the response after high pass filtering, illustrating the increase in membrane current noise during channel deactivation. Scale bar 50 pA and 20 s. ***B,*** A representative current-variance relationship is superimposed on the fit of equation 1 to the data (*Methods*). ***C,*** Photomicrograph of a cultured hippocampal neuron isolated from 129X1/Svj GluA1-S831A knock-in mice (DIV 21; scale bar: 20 µm). ***D,*** PKC enhances γ_{MEAN} of native AMPA receptors in cultured hippocampal neurons from GluA1-S831A knock-in mutant mice (mean ± SEM). * $p<0.01$ Student's unpaired *t*-test. The number of patches per condition is given in parentheses. ***E,*** Co-expression of PKC increases phosphorylation of the GluA1 C-terminus at Ser818, Ser831 and Thr840, as shown by western blot analysis using phospho-specific antibodies. Quantification of six independent experiments normalized to control values yields significant increases in phosphorylation for Ser831 (control =1.0, PKC = 3.68 ± 0.94 fold, $p<0.05$) and Thr840 (PKC = 2.25 ± 0.58 fold, $p<0.05$). Ser818 was not quantified because there is no basal signal in the absence of PKC, so the fold increase in phospho-Ser818 approaches infinity.

Molecular Pharmacology Fast Forward. Published on January 22, 2014 as DOI: 10.1124/mol.113.091488
This article has not been copyedited and formatted. The final version may differ from this version.

Figure 2. Phosphomimetic mutations do not affect the glutamate EC_{50} at GluA1. ***A,*** Representative whole-cell current trace from a HEK cell expressing GluA1-LY-AAAA receptors. Black boxes above trace represent agonist application time, with concentrations indicated above (in μM). Scale bar 500 pA and 5 s. ***B,C,*** Concentration-response relationships were determined with glutamate concentrations ranging from 0.3 μM to 1000 μM for each GluA1 mutant receptor expressed in HEK cells. Composite data were plotted on a logarithmic scale and fitted with the Hill equation. Representative current traces are shown from outside-out patches excised from HEK cells transfected with the indicated non-desensitizing GluA1-L497Y (***D***) or desensitizing GluA1-Leu497 (***E***), held at -60 mV. ***D,*** Scale bars are 50 pA and 50 ms for all GluA1-LY receptors except for GluA1-LY-EAAA (25 pA and 50 ms). ***E,*** Scale bars for WT receptors are 50 pA and 2 ms for all except GluA1-WT-AAAA (100 pA and 2 ms).

Figure 3. Structural determinants of C-terminal regulation of conductance.

A, Summary of results from glutamate-scan experiments in which all residues between GluA1- Lys813 and -Thr840 were individually mutated to glutamate and weighted mean conductance (γ_{MEAN}) was determined from variance analysis. Groups of 3 consecutive residues were paired with GluA1 controls for each experiment and a statistical test was performed on these subgroupings to assess the changes in γ_{MEAN} (see *Methods*). * $p<0.01$, one-way ANOVA, Tukey's post-hoc test. ***B,*** Linear representation of the GluA1 subunit, indicating C-terminal residues at which stop codons were inserted to truncate the receptor. Represented above the C-terminal amino acid sequence is a schematic of the two domains, the membrane proximal region (C1 in light red) and the more distal C-terminal domain (C2 in

Molecular Pharmacology Fast Forward. Published on January 22, 2014 as DOI: 10.1124/mol.113.091488
This article has not been copyedited and formatted. The final version may differ from this version.

green). C1 and C2 are connected via a glycine-rich flexible linker (black). The same color-coding is applicable to the residues in red, black and green. ***C,*** Summary of γ_{MEAN} values from a series of GluA1-AEAA truncation mutants (mean ± SEM) with stop codons inserted in place of the indicated amino acid codons (* $p<0.05$ compared to full-length GluA1-AAAA, one-way ANOVA, Tukey's post hoc test). The number of outside-out patches per condition is in parentheses in all panels.

Figure 4. GluA1 C-terminal domain structural model. ***A,*** (*Left panel*) The antagonist-bound GluA2 crystal structure illustrates the extracellular and membrane bound regions of the GluA1 receptor (grey). Attached to the intracellular side of a single subunit is a molecular model of the predicted structure of the C-terminal domain. (*Right panel*) Expanded view of the predicted C-terminal domain structural model. C1 is comprised of two helices, in green, the first helix contains GluA1 Ser818 whereas the second helix is flanked by GluA1 Ser831 and Thr840 (3 phosphorylation sites are highlighted in blue). The C_α atoms of the critical G-A-G-A residues required for the phospho-Ser831 and phospho-Thr840 mediated conductance increase are also highlighted as yellow spheres (1.2 × van Der Waals radii). The glycine-rich flexible linker region C-terminal to GluA1-Ser850 is shown in orange. Only the initial portion of the C-terminal domain "C2," required for the phospho-Ser818 mediated conductance increase, is shown. The proximal C1 region is absent. ***B,*** The Phyre2 secondary structural prediction is compared to the helical elements detected by NMR analysis of a peptide corresponding to residues 828-849 (PQQSINEAIRTSTLPRNSGAGA). Cylinders indicated alpha-helices with the remainder of the sequence predicted to be disordered loops.

Molecular Pharmacology Fast Forward. Published on January 22, 2014 as DOI: 10.1124/mol.113.091488
This article has not been copyedited and formatted. The final version may differ from this version.

C, Natural abundance $^{1}H,^{15}N$-HSQC spectrum for the unphosphorylated peptide (black) with the spectrum for the phosphorylated peptides in red. This two-dimensional spectrum shows through bond correlations between ^{1}H and ^{15}N, and provides chemical shift information for both. The spectrum includes the backbone NH for each amino acid in the peptide except proline and sidechain (sc) NH (Arg) and NH_2 (Asn or Gln). Because very little change in the NH_2 resonances was observed for the spectrum of the peptide phosphorylated at Ser845, the peaks were not labeled (see labels for the unphosphorylated peptide in the spectrum on the right). The spectra were obtained at 500 MHz for proton using a cryogenic probe. A total of 128 complex points were obtained in the ^{15}N dimension and 1024 in the ^{1}H dimension.

Figure 5. Phosphorylation at Ser831 alters C-terminal structure. ***A,*** (*Top panel*) The twenty lowest energy structures calculated for the peptide phosphorylated on Ser831 are superimposed. The structures were aligned using the backbone atoms between Ile832 through Arg837 which form helical elements. (*Bottom panel*) The twenty lowest energy structures calculated for the unphosphorylated peptide are shown. Alignment was done as for the unphosphorylated peptide. ***B,*** Chemical shift changes are shown for wild type peptide versus Ser831 phosphorylated (*left panel*) or Ser845 phosphorylated (*right panel*). The red bar indicates the phosphorylated serine. For $\Delta C\alpha$ and $\Delta H\alpha$, the phosphorylated peptide chemical shift was subtracted from the unphosphorylated chemical shift. The value for ΔN-HN was determined as:

$$\Delta N - HN = \sqrt{\frac{\Delta N^2}{10} + \Delta HN^2}$$

where ΔN is the difference in the nitrogen shift, ΔHN is the shift in the nitrogen proton.

Molecular Pharmacology Fast Forward. Published on January 22, 2014 as DOI: 10.1124/mol.113.091488
This article has not been copyedited and formatted. The final version may differ from this version.

Table 1: Phosphomimetic mutations increase γ_{MEAN} and EC_{50} of GluA1 receptors.

Receptor	γ_{MEAN} (pS)	P_O	n	EC_{50} (μM)	Hill slope	n
GluA1-LY-AAAA	10.1 ± 0.7	0.67 ± 0.05	17	7.6 ± 1.0	1.9 ± 0.2	5
GluA1-LY-EAAA	13.9 ± 0.7 *	0.73 ± 0.04	15	7.1± 1.1	1.9 ± 0.1	4
GluA1-LY-AEAA	14.9 ± 1.0 *	0.78 ± 0.04	15	9.3 ± 0.9	1.9 ± 0.2	4
GluA1-LY-AAEA	13.9 ± 0.9 *	0.72 ± 0.05	17	6.4 ±1.1	1.8 ± 0.2	5
GluA1-LY-AAAE	8.0 ± 0.8	0.91 ± 0.11 **	14	--	--	--
GluA1-LY-EEAA	13.3 ± 0.9 *	0.64 ± 0.03	15	--	--	--
GluA1-LY-EAEA	14.3 ± 1.4 *	0.67 ± 0.02	13	--	--	--
GluA1-LY-AEEA	13.0 ± 0.6 *	0.67 ± 0.03	14	--	--	--
GluA1-LY-EEEA	12.3 ± 0.8 *	0.69 ± 0.03	14	--	--	--

Weighted mean unitary conductance (γ_{MEAN}) and P_O were determined using variance analysis of current responses obtained from outside out patches from HEK cells transfected with indicated mutant AMPA receptors; all subunit cDNAs contain GluA1-L497Y to minimize AMPA receptor desensitization. Values are mean ± SEM. Holding potential was -60 mV; * $p<0.05$ significantly different from GluA1-LY-AAAA (one-way ANOVA, Tukey's post hoc test). γ_{MEAN} values for mutant receptors containing a single phosphomimetic mutation were not significantly different from that of receptors with the phosphomimetic mutation at the same site as well as at a second residue (**$p<0.05$ by Student's *t*-test). Measurements for concentration-effect curves were made from whole-cell patch-clamp recordings from HEK cells transfected with non-desensitizing phosphomutant GluA1-L497Y receptors; cells were held at -60 mV. Data for each cell were fitted with the Hill equation to determine slope and

Molecular Pharmacology Fast Forward. Published on January 22, 2014 as DOI: 10.1124/mol.113.091488
This article has not been copyedited and formatted. The final version may differ from this version.

EC_{50} (± SEM). GluA1-LY with wild type C-terminus had an EC_{50} for glutamate of 11±1.4 μM (Hill slope 1.8, n=4). *n* is the number of patches or cells.

Molecular Pharmacology Fast Forward. Published on January 22, 2014 as DOI: 10.1124/mol.113.091488
This article has not been copyedited and formatted. The final version may differ from this version.

Table 2. Phosphomimetic mutations do not change GluA1 response time course

DEACTIVATION

Receptor	10-90% Rise (ms)	$\tau_{f\text{-}deact}$(ms)	$\tau_{s\text{-}deact}$(ms)	% $\tau_{f\text{-}deact}$(ms)	SS/PK	n
GluA1-LY-AAAA	1.04 ± 0.09	15.7 ± 1.6	198 ± 23	87%	0.92	6
GluA1-LY-EAAA	0.95 ± 0.4	15.2 ± 2.2	129 ± 31	86%	0.90	5
GluA1-LY-AEAA	1.06 ± 0.3	18.0 ± 6.8	137 ± 15	77%	0.89	5
GluA1-LY-AAEA	0.67 ± 0.2	17.3 ± 5.0	158 ± 12	85%	0.92	5

DESENSITIZATION

Receptor	10-90% Rise (ms)	$\tau_{f\text{-}desens}$(ms)	$\tau_{s\text{-}desens}$(ms)	% $\tau_{f\text{-}desens}$(ms)	SS/PK	n
GluA1-AAAA	0.41 ± 0.03	2.2 ± 0.6	49 ± 26	88%	0.02	5
GluA1-EAAA	0.42 ± 0.04	3.0 ± 0.4	48 ± 15	85%	0.03	6
GluA1-AEAA	0.42 ± 0.09	2.9 ± 0.4	55 ± 13	89%	0.02	5
GluA1-AAEA	0.61 ± 0.01	2.5 ± 0.2	42 ± 11	86%	0.02	5

Current responses were recorded from outside-out membrane patches excised from HEK cells transfected with the indicated non-desensitizing GluA1-LY or desensitizing GluA1 receptors. Rise time is measured as duration of time it takes for the response to increase from 10 to 90% of the maximal amplitude. $\tau_{f\text{-}deact}$ is the fast and $\tau_{s\text{-}deact}$ is the slow time constant for a dual exponential function fitted to the relaxation after agonist removal. $\tau_{f\text{-}desens}$ is the fast and $\tau_{s\text{-}desens}$ is the slow time constant for a dual exponential component fitted to the relaxation during continued agonist application. SS/PK represents the ratio of the steady state (SS) to the peak (PK) current amplitude. None of the mean values were significantly different (one-way ANOVA).

Molecular Pharmacology Fast Forward. Published on January 22, 2014 as DOI: 10.1124/mol.113.091488
This article has not been copyedited and formatted. The final version may differ from this version.

Table 3. Structural determinants of phosphomimetic effects on conductance

Receptor	γ_{MEAN} (pS)	P_O	n
GluA1-S818E-Δ846	8.9 ± 1.5	0.67 ± 0.02	6
GluA1-S818E-Δ850	8.0 ± 0.5	0.70 ± 0.05	8
GluA1-S831E-Δ846	9.0 ± 1.0	0.66 ± 0.07	6
GluA1-S831E-Δ850	14.3 ± 0.7 *	0.76 ± 0.03	10
GluA1-T840E-Δ846	9.1 ± 0.5	0.68 ± 0.04	11
GluA1-T840E-Δ850	14.7 ± 0.9 *	0.75 ± 0.03	7

Stop codons were inserted into GluA1-LY-EAAA, -AEAA , or -AAEA mutant receptors before and after the G-A-G-A region (residues 846-849, Figure 3,4). γ_{MEAN} and P_O values were compared across all truncation mutants by one-way ANOVA with Tukey's post hoc test. * $p<0.05$; n indicates number of patches per condition.

Molecular Pharmacology Fast Forward. Published on January 22, 2014 as DOI: 10.1124/mol.113.091488
This article has not been copyedited and formatted. The final version may differ from this version.

Table 4: NMR and refinement statistics for unphosphorylated and phosphorylated peptides.

	Phosphorylated	Unphosphorylated
NMR distance and dihedral constraints		
Distance constraints		
Total NOE	161	117
Intra-residue	92	54
Inter-residue		
Sequential ($\|i - j\| = 1$)	56	53
Medium-range ($\|i - j\| < 4$)	13	10
Structure statistics		
Violations (mean and s.d.)		
Distance constraints (Å)	0.13 ± 0.19	0.09 ± 0.15
Max. distance constraint violation (Å)	1.40	1.29
Deviations from idealized geometry		
Bond lengths (Å)	1.29e-3 ± 0.18e-3	1.15e-3 ± 0.12e-3
Bond angles (º)	0.42 ± 0.01	0.45 ± 0.01
Impropers (º)	0.27 ± 0.003	0.27 ± 0.002
Average pairwise r.m.s. deviation (Å)		
Heavy (resid 5-10, 20 structures)	0.84 ± 0.16	0.82 ± 0.34
Backbone (resid 5-10, 20 structures)	1.61 ± 0.16	1.69 ± 0.60

Molecular Pharmacology Fast Forward. Published on January 22, 2014 as DOI: 10.1124/mol.113.091488
This article has not been copyedited and formatted. The final version may differ from this version.

Figure 1

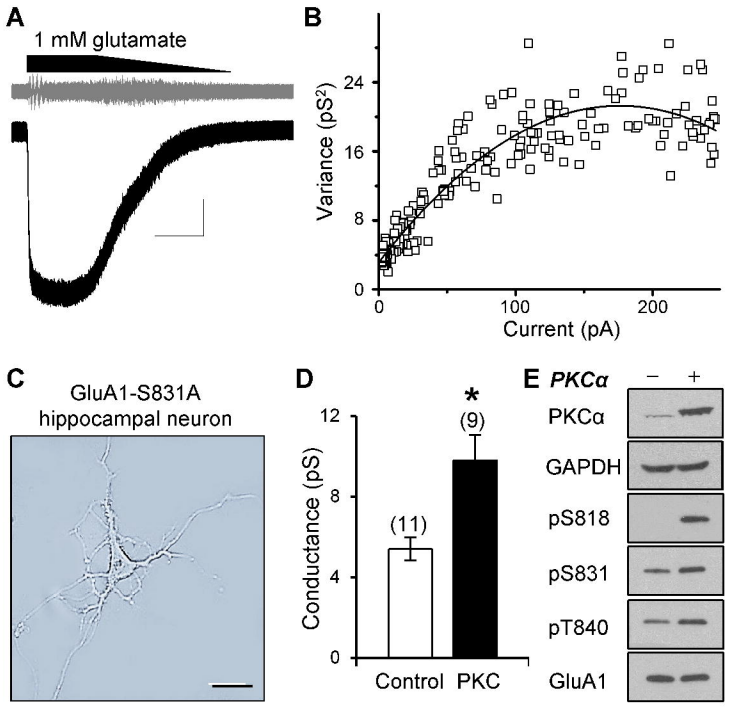

Molecular Pharmacology Fast Forward. Published on January 22, 2014 as DOI: 10.1124/mol.113.091488
This article has not been copyedited and formatted. The final version may differ from this version.

Figure 2

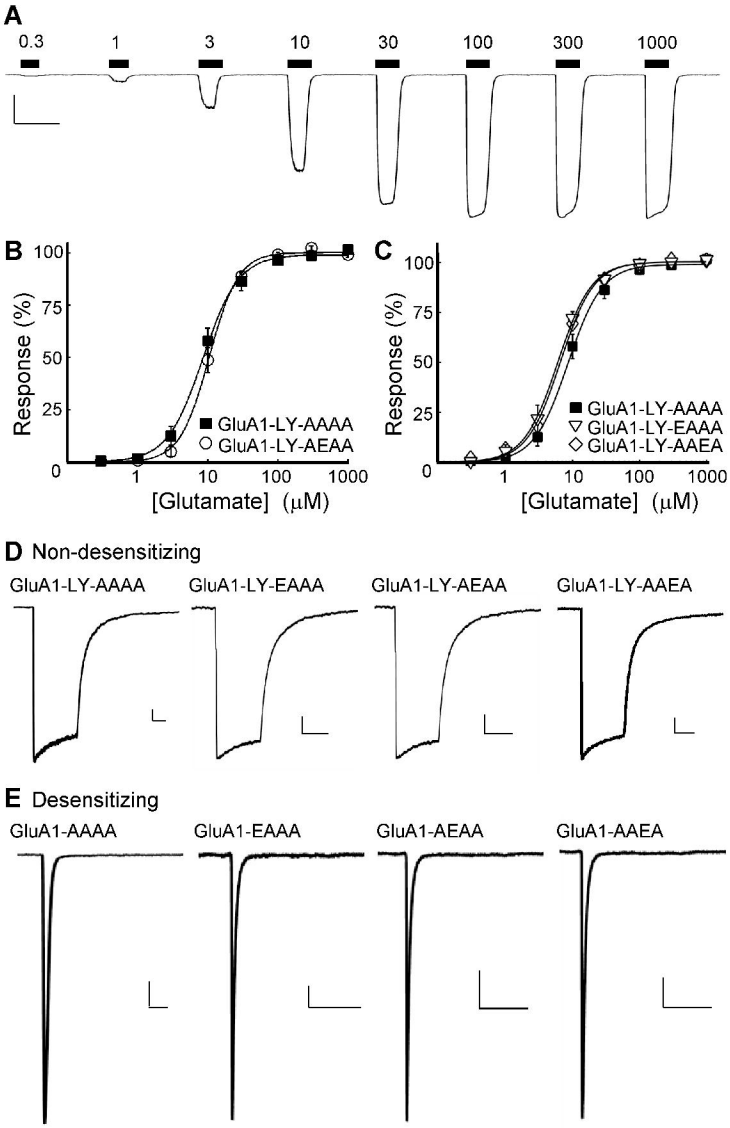

Molecular Pharmacology Fast Forward. Published on January 22, 2014 as DOI: 10.1124/mol.113.091488
This article has not been copyedited and formatted. The final version may differ from this version.

Figure 3

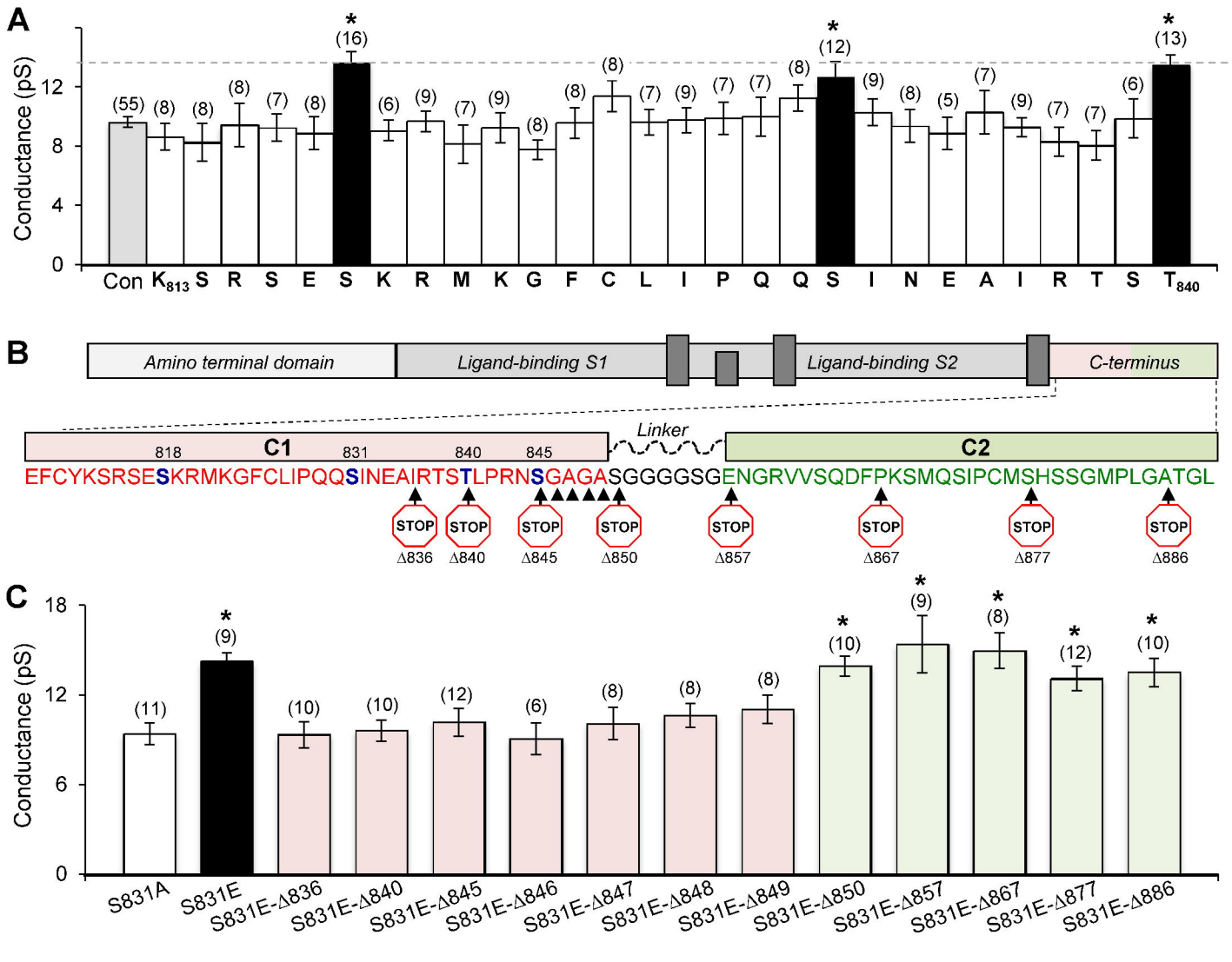

Molecular Pharmacology Fast Forward. Published on January 22, 2014 as DOI: 10.1124/mol.113.091488
This article has not been copyedited and formatted. The final version may differ from this version.

Figure 4

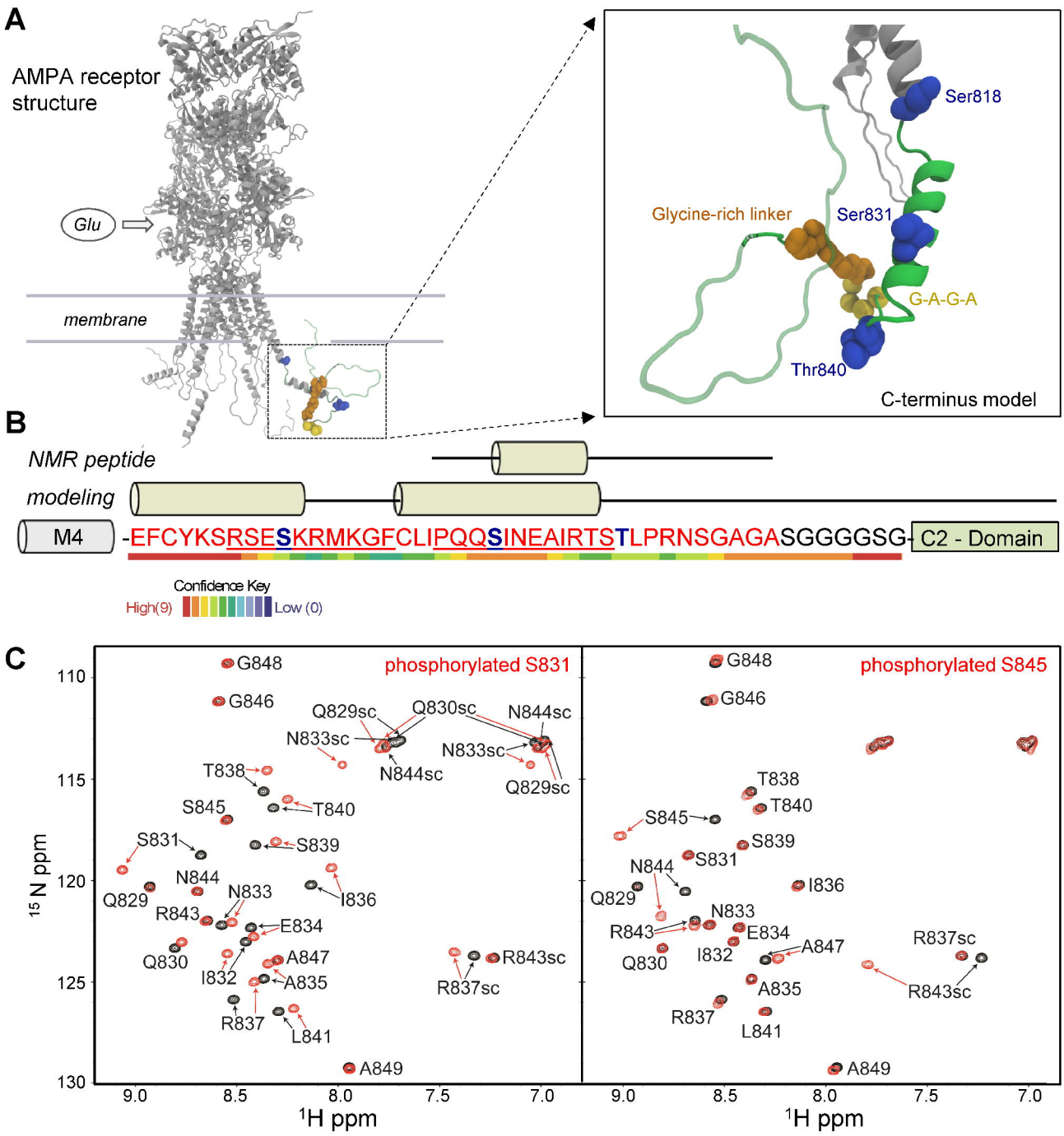

Molecular Pharmacology Fast Forward. Published on January 22, 2014 as DOI: 10.1124/mol.113.091488
This article has not been copyedited and formatted. The final version may differ from this version.

Figure 5